Optimization of thrust based on vacuum arc by means of pulsed magnetic field*

Evgeny Nefedtsev

Larisa Zjul'kova

Institute of High Current Electronics SB RAS
2/3 Academichesky Ave., 634055, Tomsk, Russia
nev@lve.hcei.tsc.ru

* This study has been supported by a grant from the Russian Science Foundation (Project No. 18-19-00270)

I. INTRODUCTION

Recently there are a lot of designs for spacecraft engines based on electric propulsion. Capabilities of the pulsed arc discharge, which has several advantages to create thrust in small and ultra-small spacecraft, have not been fully studied. Important advantages include the possibility of using a condensed working medium (including one with a significant atomic mass), high supersonic plasma flow rates, and an ability to adjust the thrust in the ~ 1–10 μN range with a sufficiently high accuracy by several independent parameters: frequency, duration and power of ignition pulses.

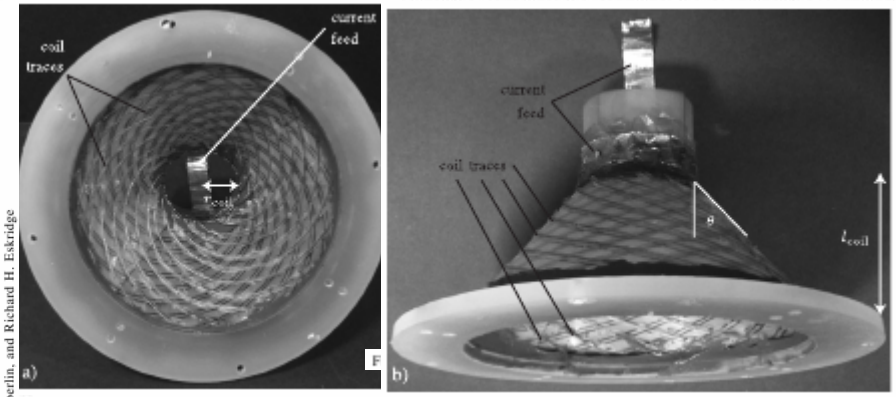

Fig. 2. Images of the 38° CTP inductive coil. (a) Front view along the axis. (b) Top view.

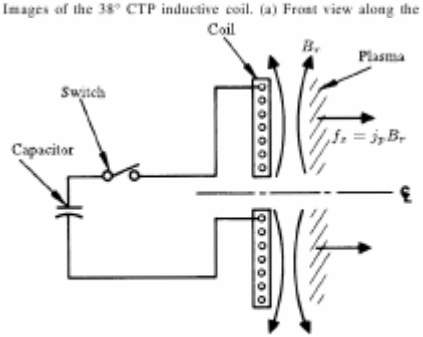

Fig. 1. Schematic of a planar pulsed inductive plasma accelerator, where j_θ is the azimuthal plasma current density and f_z is the axial Lorentz body force (after [6]).

Single- and Repetitive-Pulse Conical Theta-Pinch Inductive Pulsed Plasma Thruster Performance

Ashley K. Hallock, Adam K. Martin, Kurt A. Polzin, *Senior Member, IEEE*, Adam C. Kimberlin, and Richard H. Eskridge

IEEE TRANSACTIONS ON PLASMA SCIENCE, VOL. 43, NO. 1, JANUARY 2015

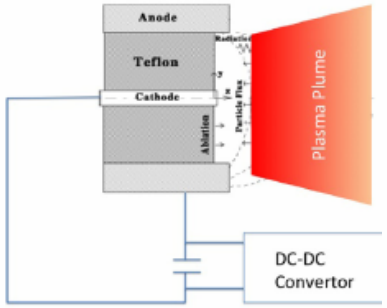

Figure 1. Schematic of the co-axial micro-PPT.

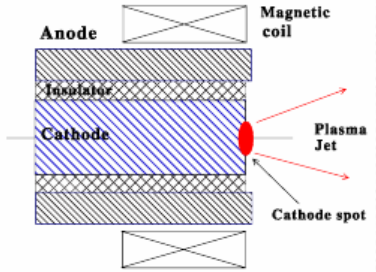

Figure 2. Schematics of the vacuum arc thruster (reproduced with

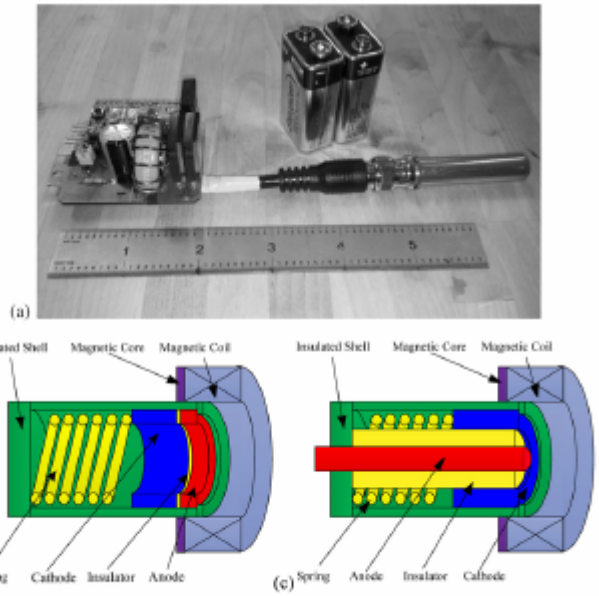

Figure 3. (*a*) μCAT with PPU. (*b*) Schematic design of the ring shape μCAT, (*c*) schematic design of co-axial electrodes μCAT.

Plasma Physics and Controlled Fusion doi:10.1088/0741-3335/57/10/14005

IOP Publishing Plasma Phys. Control. Fusion 57 (2015) 014005 (10pp)

Electric propulsion for small satellites

Michael Keidar, Taisen Zhuang, Alexey Shashurin, George Teel, Dereck Chiu, Joseph Lukas, Samudra Haque and Lubos Brieda

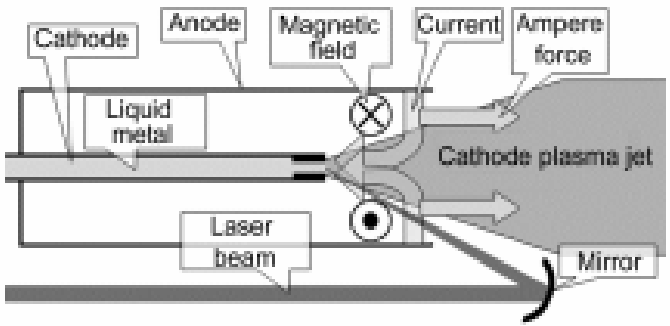

Fig. 1. Concept of a hybrid dual-mode plasma thruster.

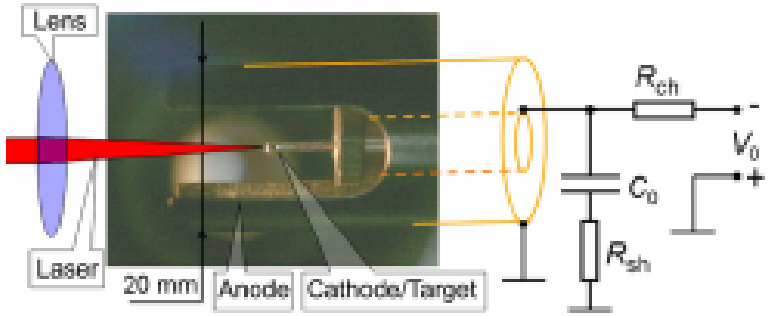

Fig. 2. Principle scheme of the experiment.

DOI 10.1007/s11182-019-01640-z

Russian Physics Journal, Vol. 61, No. 11, March, 2019 (Russian Original No. 11, November, 2018)

THE CONCEPT OF A HYBRID PULSED PLASMA THRUSTER FOR SMALL-SIZE SPACE SATELLITES

S. A. Popov, E. L. Dubrovskaya, and A. V. Batrakov

UDC 533.9.03, 53.06

As a rule, disadvantages of the vacuum arc plasma source include erosion of electrodes, which reduces engine lifetime. However this problem can be solved by means of a liquid-phase metal propellant automatically fed to the discharge zone through a steel capillary.

The principal disadvantage of the high-current vacuum arc plasma is its wide spray pattern resulting in large momentum losses in radial direction and, consequently, to low propulsion efficiency. This disadvantage can be eliminated by plasma compression by an external magnetic field. Considering the pulsed mode of vacuum-arc plasma generation, it is more appropriate in this case to use the inductive interaction between the plasma and the magnetic field. Such interaction is realized, for example, in pulsed gas-plasma engines. However, taking into account the initially high plasma expansion rate, it is not so much about its inductive acceleration, but rather about correction the angular diagram of its expansion. In addition to search for the optimal spatial configuration of the magnetic field, the problem of optimizing the delay of the magnetic field pulse relative to the arc ignition pulse also is of high importance.

In this paper, based on numerical simulation, estimates of configurations and parameters of the magnetic field pulse are given, providing significant changes in the traction force of the vacuum arc plasma source. These estimates may also be applicable to a plasma source based on pulsed overheating of a material by a laser beam.

II. CALCULATION METHODS AND MATHEMATICAL MODEL

The simulation was performed using the Comsol Multiphysics (CM) version 5.4 computing environment. Given that the basis of the “Plasma” module in CM is a drift-diffusion model, which is more suitable for describing properties of low-gradient technological plasma with a high background of neutrals, the “Computation fluid dynamics” (CFD) module and the magneto-hydrodynamic (MHD) theoretical model of the plasma were used in the work. In this model, the plasma is considered as an unitary quasi-neutral liquid with some effective volume density ρ, directed velocity *V*, pressure *P*, and effective temperature *T*. First pair of values is determined mainly by the concentration of ions and their average flow rate. The second pair of values is determined by parameters of the electronic plasma subsystem.

We will neglect the inter-electrode component of the current density, which is almost all concentrated in the small spark zone. Therefore, we‘re going to assume that the current density J and the electric field strength E in the main part of the device’s volume are determined by the induced vortex components. Based on two blocks: “Non-Isothermal Flow” from the CFD module and “Magnetic Fields”, we obtain a system of equations that corresponds to the quasi-stationary MHD model of simplest plasma .

$$\frac{\partial \rho}{\partial t} + \nabla \cdot (\rho \mathbf{V}) = 0\,, \qquad (1)$$

$$\rho \frac{\partial \mathbf{V}}{\partial t} + \rho(\mathbf{V} \cdot \nabla)\mathbf{V} = -\nabla\left[P\mathbf{I} + \mu\left(\nabla\mathbf{V} + (\nabla\mathbf{V})^T\right) - \frac{2}{3}\mu(\nabla \cdot \mathbf{V})\mathbf{I}\right] + \mathbf{F}\,, \qquad (2)$$

$$\rho C\left(\frac{\partial T}{\partial t} + \mathbf{V}\nabla T\right) = \nabla \cdot (k\nabla T) + Q\,, \qquad (3)$$

$$\rho = \frac{MP}{ZkT}\,, \qquad (4)$$

$$\nabla \times \mathbf{B} = \mu_0 \mathbf{J}\,, \qquad (5)$$

$$\mathbf{J} = \sigma\mathbf{E} + \sigma\mathbf{v} \times \mathbf{B} + \mathbf{J_e}\,, \qquad (6)$$

$$\mathbf{B} = \nabla \times \mathbf{A}\,, \qquad (7)$$

$$\mathbf{E} = -\frac{\partial \mathbf{A}}{\partial t}\,. \qquad (8)$$

Continuity (1), Navier-Stokes (2), and heat balance (3) equations describe the dynamics and the heat function of each unit of the medium volume in time *t*. In this case, the “external” Lorentz force is also added in the right-hand side of equation (2) to the pressure and viscosity forces (μ is the viscosity coefficient) acting on a unit element of the plasma volume:

$$\mathbf{F} = \mathbf{J} \times \mathbf{B}\,. \qquad (9)$$

Equation of state (4) describes plasma as an ideal neutral gas in which the pressure P is proportional to the temperature: $P = n_e kT$, where k is the Boltzmann's constant; $n_e = Zn_i = Z\rho/M$ is the electron concentration; n_i is the ion concentration, Z and M are the average values of the charge number and the mass of the plasma ion, respectively.

The heat balance equation (3) accounts Joule heat

$$Q = J^2/\sigma \quad , \tag{10}$$

where σ is the plasma conductivity, it is mainly determined by scattering of electrons by ions in the magnetic field:

$$\sigma = \frac{e^2 n_e}{m\nu_{ei}}\left(1 - \frac{\alpha'_1 \cdot x^2 + \alpha'_0}{x^4 + \delta_1 \cdot x^2 + \delta_0}\right)^{-1} \quad . \tag{11}$$

As far as the azimuthal component of the current was considered dominant in the model, the conductivity component orthogonal to magnetic field lines was taken into account. In expression (11), the term enclosed in brackets is an amendment, including action of the magnetic field, to the Spitzer conductivity and the value $x = (eB/m)/\nu_{ei}$ is the ratio of the Larmor frequency of electrons to the average frequency of their scattering at Coulomb centers:

$$\nu_{ei} = \frac{4 \cdot (2\pi)^{1/2} e^4 Z^2}{3(4\pi\varepsilon_0)^2} \frac{m^{1/2} n_i}{(kT)^{3/2}} \Lambda_{ei} \quad . \tag{12}$$

Coefficients $\alpha'_1 = 5.523$; $\alpha'_0 = 0.5956$; $\delta_1 = 10.8$; $\delta_0 = 1.0465$ correspond to the case $Z = 2$. The Coulomb logarithm Λ_{ei} can be expressed as

$$\Lambda_{ei} = \ln\left(2.415 \cdot 10^{41}\right) + 1.5\ln\left(kT_e\left[\mathrm{J}\right]\right) - 0.5\ln\left(n_i\left[\mathrm{m}^{-3}\right]\right) \quad . \tag{13}$$

The system of equations describing the magnetic field includes Ampere's law (5), generalized Ohm's law (6) and Faraday's law (7)–(8). In CM, these equations are solved with respect to the components of the vector potential **A**. The value $\mathbf{J_e}$ in the “Magnetic Fields” interface describes external currents. It is convenient to associate the current component due to the plasma pressure gradient with this quantity $\mathbf{J_e}$ in the combined model and put

$$\mathbf{J_e} = \frac{\nabla n_e kT}{e n_e} \approx \frac{kT}{e} \nabla \ln P \quad . \tag{14}$$

III. TASK PARAMETERS

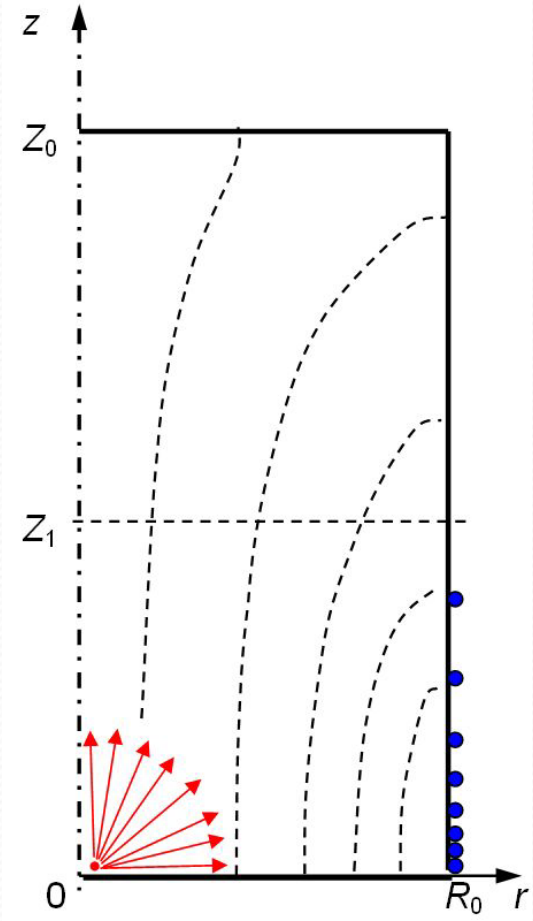

Fig. 1. The computational domain with the point plasma source and the electromagnetic coil located on the side surface of the accelerator. The arrows schematically show directions of plasma expansion, and dashed lines show magnetic field lines.

The task was solved in the axial-isotropic approximation, taking into account the occurrence of azimuthal components of vector quantities. The calculated domain was a cylinder of the radius R_0 = 30 mm and the height Z_0 = 60 mm (Fig. 1). Boundaries of the area, except for the part of the cylinder's base (z = 0, r < 10 mm) adjacent to the plasma source, were as considered remote. The condition of free outflow of the plasma liquid and fixation of the plasma temperature at the low level T_0=600 K (which is by over an order of magnitude lower than the temperature of the plasma source) was formulated at these boundaries. The plasma source with ignition on the dielectric surface was simulated by a thin ring with a diameter of 2 mm and located at a height of 0.5 mm above the base surface (Fig. 1).

Calculations simulated a pulse-periodic mode within three periods. The initial condition of absolute emptiness is unacceptable, so at time t = 0 the volume of the computational area was considered as cold plasma filled with the uniform pressure of 1 Pa at temperature of 600 K. By the time of beginning of the second and subsequent periods, this problem had been disappeared, because the area had been filled with the residual plasma generated during the previous period. During the initial period of 0 < t < 50 μs of the first cycle, the plasma source temperature was also gradually set at 8000 K and a pulsed plasma source was switched on with the pressure level of the order of tens kilo-pascals.

IV. RESULTS

Configurations of electromagnetic systems were considered in the form of the surface azimuth current with varying distribution that circulated 1) along the lower part of the cylindrical wall within ($r = R_0$; $z < Z_1$) and 2) along the cylinder base within ($r > 10$ mm; $z = 0$), as well as 3) the azimuthal current uniformly distributed within certain variable volume inside the device ($r > 10$ mm; $z < Z_1$).

Calculations have shown that for all of these magnetic field sources, the maximum of the traction pulse is reached at the limit "concentration of the electromagnetic coil turns" to the angular point of the computational domain ($r = R_0$; $z = 0$). Herewith the optimal delay of the magnetic field pulse Δt relative to the plasma source pulse is approximately equal to the time of plasma boundary propagation to the region of localization of the magnetic coil.

This result is natural due to high gradients of the expanding plasma. The magnetic field with reasonable values of magnetic flux density and frequency can penetrate only into peripheral layers of the plasma, providing the corrective effect on the particle flow. With that the maximum steepness of magnetic flux density rise dB/dt should correspond to the time moment at which near the wall the maximum plasma density is reached. The important condition for the optimum is to switch off the plasma source until the magnetic field disappears, as, for example, shown in Fig. 2.

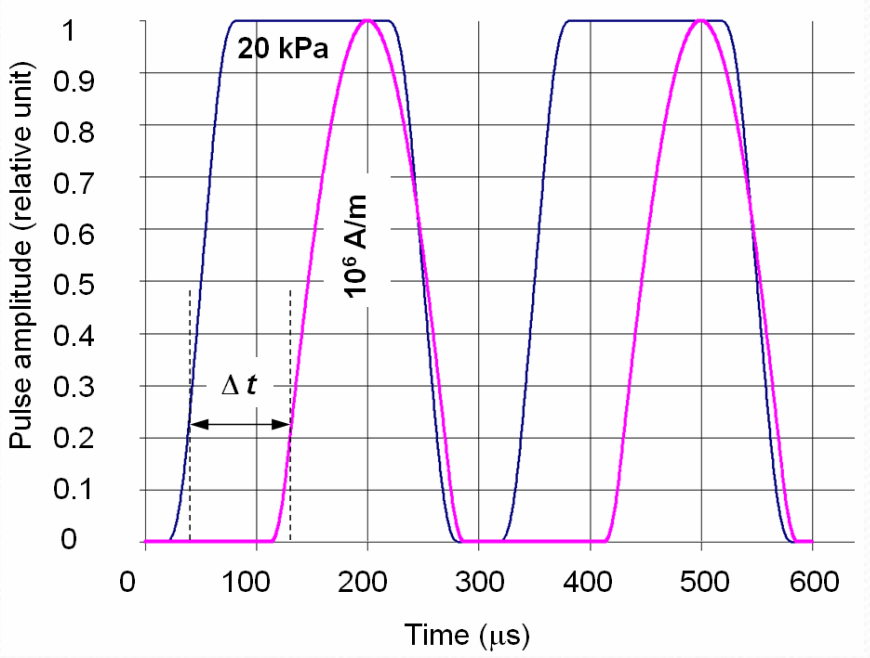

Fig. 2. Normalized pulses of the plasma source and the magnetic field source. The numbers in the figure indicate the order of amplitudes in the vicinity of which thrust parameters were optimized.

In fact, the removal of the magnetic field under conditions of a continuously functioning plasma source leads to the appearance of inductive currents of the opposite direction with respect to those that occurred during the rise front. As a result, the part of the thrust impulse "won" at the stage of field growth will be compensated, and in general the effect will be close to zero. These considerations are also confirmed by calculation of the traction force (15) as a function of time $F_T(t)$.

The thrust was characterized by the force F_T, with which the plasma flow acts in the direction of the source axis on an imaginary surface surrounding the computational domain. It was accepted

$$F_T = \int_{S_1} \rho V V_z dS \qquad (15)$$

where S_1 is upper part of the boundary surface ($r \le R_0$, $z = Z_0$) U ($r = R_0$, $Z_1 \le z \le Z_0$); V_z is the projection of the flow velocity on z axis.

The plane $z = Z_1 = 30$ mm determined the conventional geometric boundary of the accelerating device, in which electromagnet's coils are situated, so the region ($z < Z_1$) was not taken into account in calculating of the traction force. Determination of the thrust force depending on time was carried out during the entire simulation procedure, as a result of which it was possible to calculate the recoil momentum and estimative optimize parameters of pulsed sources of the plasma and the magnetic field by this value

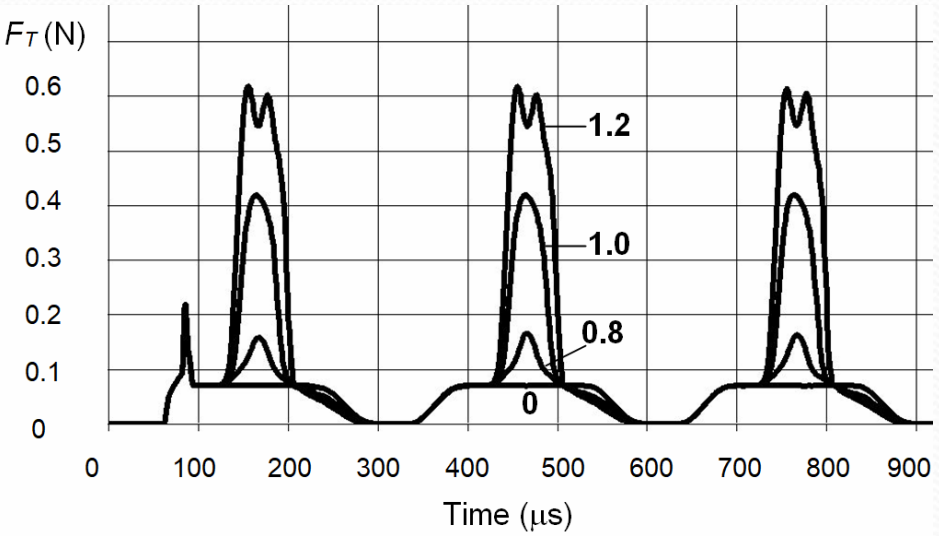

Fig. 3. Dependences of traction force on time at various values of I_0 of short coil $z_0 = 0.5$ mm (values are indicated on the graph in mega-amperes per meter).

For example, we consider the first type magnetic field source (see above) characterized by distribution

$$I = I_0 \exp[-(z/z_0)^2], \qquad (16)$$

where $I = i \cdot N$ is the linear azimuthal current density (A/m); i is the current in the coil (A); N is the density of turns (m^{-1}), I_0 is the maximum value of the current density at the point ($z = 0$; $r = R_0$); z_0 is the optimization parameter that determines the non-uniformity of the turns in the coil (see Fig. 1).

Fig. 3 shows dependences F_T (t) for various values of the current amplitude in the coil with the parameter $z_0 = 5$ mm (that is, which is actually concentrated at the bottom of the computational domain). The first sharp peak at beginning of the first cycle is due to artificial initial conditions (see Section III): the formation of velocity field is attended with a density wave in the initially uniformly distributed rarefied plasma. The establishment of the constant level of pressure force of 70 mN corresponds the filling of volume by arc plasma. For a duration of the plasma source operation of 200 μs, this value corresponds to the momentum of $14 \cdot 10^{-6}$ N·s.

The effect of the magnetic field becomes noticeable at the current amplitude in the magnetic field source of the order of 10^3 ampere-turns. Against the background of stationary thrust, the bell-shaped pulse appears with a maximum shifted by 20 μs relative to the maximum dI/dt (Fig.3). The shift is caused by the time of transfer of the perturbation to upper part of the boundary surface S_1. With a current amplitude of $i = 5.2 \cdot 10^3$ ampere-turns (respectively, $I_0 = 1.2 \cdot 10^6$ A/m), the effect becomes strong, passing to instability.

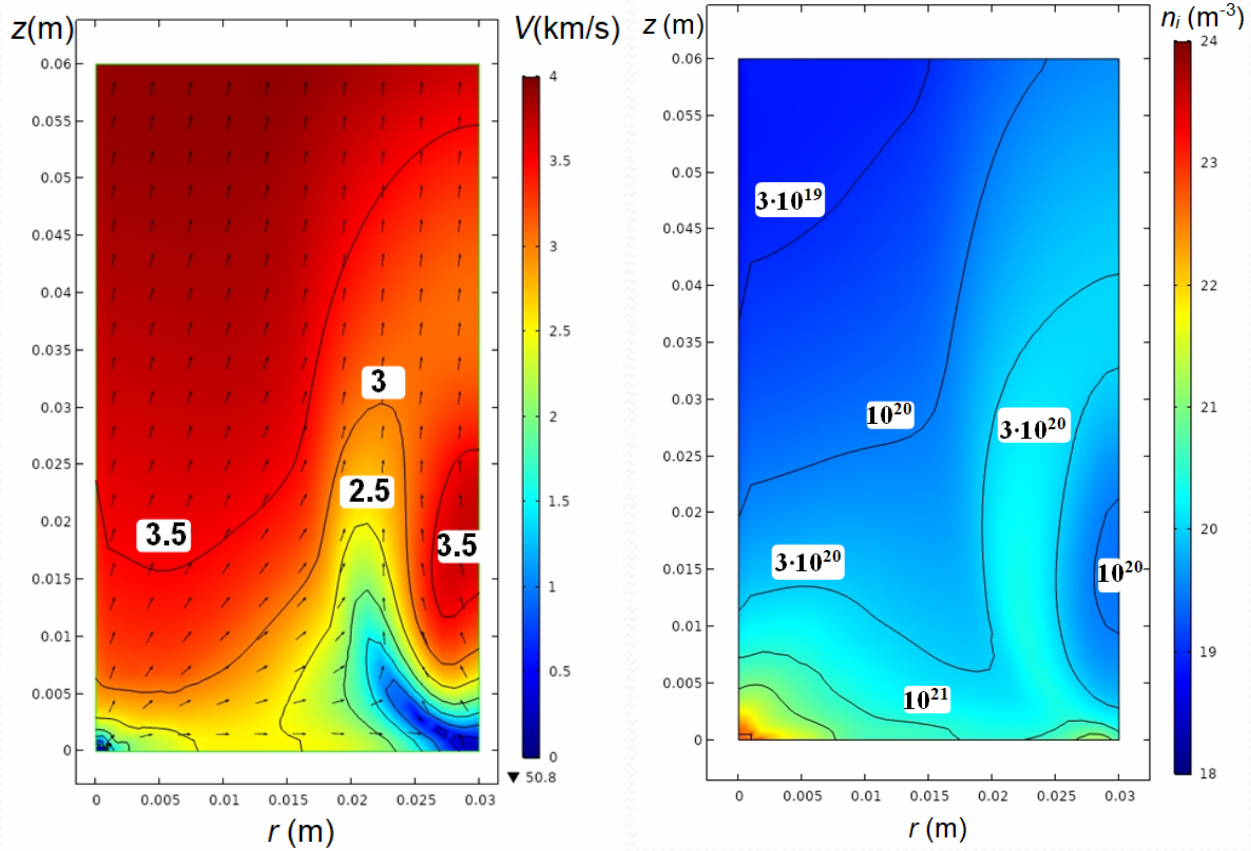

(a) (b)

Fig. 4. Fields of velocities (a) and concentration (b) of plasma ions at the time 450 μs at coil current increase to the amplitude of 6/N kA. Numbers indicate speeds in km/s and concentrations in m^{-3}.

The shape of the impulse of the traction force becomes complex in proximity the stability threshold: to the main maximum, one more maximum is added, time-shifted by 40 μs relative to the maximum dI/dt. The cause for complicated influence of the magnetic field on traction device parameters can be understood based on the analysis of plasma characteristics during periods of the maximum dI/dt (or dB/dt). Fig. 4 shows the fields of ion velocity and concentration (from the calculation of the average mass of an atom In–Ga eutectic M = $9.87 \cdot 10^{-26}$ kg = 59 AM and the average charge number Z = 2) at the time of 450 μs at $I_0 = 1.2 \cdot 10^6$ A/m.

As follows from Fig. 4, there is a sharp deceleration of the plasma flow in the radial coordinate direction during this period, as a result the peripheral part of the plasma thickens (Fig. 4,b), keeping the magnitude of *z*-component of the velocity. Thus, the first maximum on the thrust force characteristic is more related to the correction of the angular diagram of plasma expansion. At the approach the critically high d*B*/d*t* value in addition to braking correction of the plasma flow direction, there is the focusing effect that forms the protuberance-like "sheet" of compacted plasma, bordering on the velocity local maximum. The peculiar domain of flux density arises, which moves to the upper boundary, reaching it within 20 μs, where "pressure sensors" record another overshoot of the mechanical pulse. Due to appearance of the local maximum in the velocity field, this component of the thrust force can be conditionally related to the inductive plasma acceleration in *z* direction. As follows from Fig. 4, the efficiency of traction increasing due to inductive acceleration in *z* direction can be commensurate with the efficiency of increasing it due to braking in *r* direction.

As shown by calculations, when the parameter z_0 increases (that is, when the coil of the magnetic field source stretches along the wall of the device), the inductive acceleration of the plasma in *z* direction is displayed on the dependence $F_T(t)$ less and less – second maximum is blurred and overlaps with the first. At the turns inhomogeneity parameter z_0 = 20 mm, the effect of adjustment and focus becomes common.

V. CONCLUSION

The calculations showed that it is possible in principle to achieve highly effective magneto-inductive correction of high-gradient plasma expansion from a localized arc source and corresponding increase in the traction pulse by several times. It can be achieved by a pulsed magnetic field with the amplitude of the Tesla fraction order and a steepness of its rise on the order of 10^4 T/s. In this case, the pulse-periodic operation mode with the delay of the front of the current pulse of the magnetic field source relative to the ignition voltage pulse of the plasma source for the time of plasma expansion within the device is required. The greatest gain in traction is created by the magnetic field source, the turns of which are laid as tightly as possible at the level of the arc source along the maximum possible radius determined by the design of the acceleration device. However, taking into account the real geometry of the anode, functional objectives of the device, requirements for reducing energy losses, the heat dissipation mode, etc. may lead to slightly different estimates of optimal parameters of the magnetic system of accelerating devices with electric traction on the short arc.

Thank you for your attention!